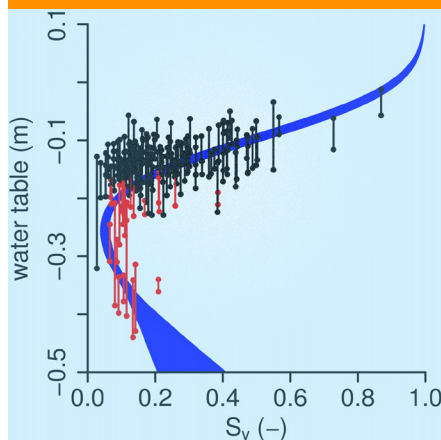


Original Research



Core Ideas

- This is a new approach for determining in situ peat soil water retention characteristics.
- It only requires data on water table changes, precipitation, and microrelief.
- Water table rises are used to invert for water retention parameters.
- Applicability is demonstrated for field data from a peatland.
- This approach should be applicable to other shallow groundwater systems.

Thünen Institute of Climate-Smart Agriculture, Bundesallee 50, 38116 Braunschweig, Germany. *Corresponding author (ullrich.dettmann@thuenen.de).

Vadose Zone J.
doi:10.2136/vzj2016.04.0029
Open access.
Received 8 Apr. 2016.
Accepted 8 Sept. 2016.

Vol. 15, Iss. 10, 2016
© Soil Science Society of America.
This is an open access article distributed under the CC BY license (<http://creativecommons.org/licenses/by/4.0/>).

Deriving Effective Soil Water Retention Characteristics from Shallow Water Table Fluctuations in Peatlands

Ullrich Dettmann* and Michel Bechtold

We have developed a novel and simple approach that can be used to derive effective in situ soil water retention characteristics from field monitoring time series in peatlands. The simplicity of the approach is given by the very limited data requirements, which comprise only precipitation, water table, and, if relevant, microrelief data. Our approach is built on two main assumptions: (i) for shallow groundwater systems, the soil moisture profile is always close to hydrostatic equilibrium; and (ii) during short time periods of high precipitation, the water storage change due to lateral fluxes is small compared with the precipitation input. Given these assumptions, the height of a water table rise due to a precipitation event mainly depends on the soil water retention characteristics, the precipitation amount, the initial water table depth, and, if present, the microrelief. In this study, this dependency was used to determine the effective van Genuchten parameters by Bayesian inversion assuming a uniform soil profile. We applied our concept to field data from a peatland with microrelief. Results indicated that observations of water table rises caused by precipitation events can contain sufficient information to constrain the soil water retention characteristics around monitoring wells in peatlands to plausible ranges. In principle, the approach should also be applicable to other shallow groundwater systems. Application limits and potential systematic errors are discussed.

Abbreviations: pdf, posterior density function; vG, van Genuchten; WRC, water retention characteristics.

The characterization of soil hydraulic properties, including their field variability and scale dependency, is an ongoing research challenge in soil science for decades (Jury et al., 2011). Still, most commonly, soil hydraulic properties are obtained for relatively small soil samples by laboratory measurements imposing steady-state (e.g., hanging water column) (Durner and Lipsius, 2005; Reynolds et al., 2002b) or transient conditions (e.g., evaporation experiments) (Dettmann et al., 2014). However, hydraulic properties obtained in the laboratory may not be representative for field conditions and often disagree with hydraulic properties determined in situ (Basile et al., 2003). One reason for this disagreement is that in the laboratory higher saturation is often achieved compared with field conditions, under which the portion of entrapped air is higher. Another reason for deviation is sample size. For practical reasons and to achieve a sufficient number of replicates, in many studies, soil sample size is chosen too small to sample a representative elementary volume of the soil heterogeneity that is characteristic for the specific soil. Additionally, samples may be disturbed by the sampling procedure, e.g., due to compaction or disturbance of the soil structure. Further, soil samples may behave differently in the laboratory than the soil under field conditions, as is the case for clay and peat that present different shrinkage characteristics once cut from the coherent soil body and root system (Mitchell, 1991; Mitchell and van Genuchten, 1992). In peatlands, shrinkage above and compression below the water table can have considerable influence on how the soil profile stores and releases water when the water table fluctuates (Price and Schlotzhauer, 1999). Further shrinkage and swelling changes the pore size distribution, and soil hydraulic properties

are thus temporally variable (Chow et al., 1992; Mapa et al., 1986). Such effects pose limitations on the transfer of laboratory parameters to the field. Therefore, for applications at the field scale, in situ measurements provide important advantages over laboratory measurements because they are more representative (Paquet et al., 1993) and obtain data in the natural environment, including interactions between different soil layers and scales (Wollschläger et al., 2009).

Several methods exist for the hydraulic characterization of a soil under field conditions. The saturated hydraulic conductivity can be measured with bail tests (Hvorslev, 1951) or by infiltration-based methods, e.g., the double-ring infiltrometer (Reynolds et al., 2002a). A tension disk or pressure ring infiltrometer can be used to obtain the unsaturated hydraulic conductivity at specific pressure heads (Ankeny et al., 1991; Basile et al., 2003). This method is applicable for low suctions (approximately more than -25 cm) (Bodhinayake et al., 2004). The direct in situ determination of the soil water retention characteristics (WRC) is limited to simultaneous measurements of water content (θ) and pressure head. Because these are point-like measurements, this approach requires an appropriate number of replicates per horizon. Additionally, measurements of θ often require soil-specific calibrations, especially for soils with high soil organic carbon contents and distinctive shrinkage and swelling characteristics (Nagare et al., 2011; Pepin et al., 1992; Shibchurn et al., 2005). An alternative to direct in situ measurements is the indirect determination of hydraulic parameters with inverse optimization using in situ measured state variables (Jadoon et al., 2012; Wollschläger et al., 2009). However, this approach requires various measurements as input (precipitation, evaporation, surface- and groundwater in- and outputs) besides the observed state variables.

In peatlands, the soil hydraulic properties are crucially influencing water table fluctuations and specific hydrological conditions and therefore physical, chemical, and biological processes (Dimitrov et al., 2010; Holden et al., 2004; Lafleur et al., 2005; McLaughlin and Cohen, 2014; Waddington et al., 2015). Unfortunately, for shallow groundwater systems, knowledge about soil WRC at the field scale is scarce due to the difficulties of common in situ methods. Infiltration methods are problematic due to the influence of the shallow water table that lowers infiltration. Furthermore, accurate in situ measurements of θ are difficult to obtain in wetlands with high soil organic carbon contents (Mortl et al., 2011), which is of concern for both the direct and inverse determination of the soil WRC. On the contrary, water table and standard meteorological data are easy to obtain and widely available for shallow groundwater systems. As mentioned above, water table depth dynamics as a response to boundary fluxes contain information about the WRC of a soil. To our knowledge, this information has not yet been exploited to inversely estimate soil the WRC.

Many kinds of landscapes with shallow groundwater tables are characterized by a distinctive microrelief that has complex effects

on hydrological processes (Van der Ploeg et al., 2012). Water table dynamics at high water tables are strongly affected by a partially inundated, uneven soil surface that increases the specific yield of the system and permits the initiation of surface runoff before the whole soil surface is inundated. Also, at lower water tables in the absence of partial inundation, the specific yield is influenced by the microrelief through the non-uniform vertical distribution of the soil volume and the resulting effect on soil water retention (Dettmann and Bechtold, 2016). Dettmann and Bechtold (2016) gave a one-dimensional analytical expression combining the soil WRC and the microrelief effect on the spatially averaged specific yield (S_y). For its application, information about the microrelief as cumulative surface elevation is needed. Besides ground-based surveys, there is an increasing availability of detailed digital elevation models from laser scanning, which can be used to characterize the microrelief.

In this study, we developed an approach to inversely estimate the soil WRC of shallow groundwater systems from frequently available data on water table fluctuations, precipitation (P), and microrelief. Instead of using a continuous soil hydrological model, we focused only on periods of stronger P events. Our approach is built on two main assumptions: (i) for shallow groundwater systems, the soil moisture profile is close to hydrostatic equilibrium before and after rain events; and (ii) during short time periods of high precipitation, the water storage change due to the divergence of lateral fluxes is small compared with the precipitation input. Given these assumptions, water table rises are directly linked to the P amounts, and the height of the water table rise depends on the soil WRC, the initial water table, and the frequency distribution of the microrelief. We applied and evaluated the approach with field data from an ombrotrophic sphagnum bog complex with shallow groundwater tables.

Materials and Methods

Theory

Assuming hydrostatic equilibrium in the soil before and after a precipitation (P) event and neglecting the water storage change due to the difference between lateral in- and outflow, the amount of P is equal to the difference of the integrals of the two soil moisture profiles, $A_{z_l, \text{soil}}$ and $A_{z_u, \text{soil}}$, of a lower (z_l) and an upper water table (z_u) (Cheng et al., 2015; Dettmann and Bechtold, 2016; Nachabe, 2002). For even surfaces and water tables below ground, the difference (ΔA_{soil}) is

$$\begin{aligned}\Delta A_{\text{soil}} &= A_{z_u, \text{soil}} - A_{z_l, \text{soil}} \\ &= \underbrace{\int_{z_l}^0 \theta(z_u - z) dz}_{A_{z_u, \text{soil}}} - \underbrace{\int_{z_l}^0 \theta(z_l - z) dz}_{A_{z_l, \text{soil}}} \\ &= \int_{z_l}^0 [\theta(z_u - z) - \theta(z_l - z)] dz\end{aligned}\quad [1]$$

where z is positive upward and zero at the mean elevation; $\theta(z_u - z)$ represents the water content at pressure head h at elevation

z , where $h = z_u - z$. Note that this does not correspond with the water content at an elevation $z_u - z$. Likewise, $\theta(z_l - z)$ represents the water content at pressure head h at elevation z , where $h = z_l - z$.

The value of ΔA_{soil} decreases with shallower water tables. When z_l and z_u are above ground, i.e., for periods of total inundation, P is equal to $\Delta z = z_u - z_l$, i.e., the height difference of two open water surfaces, further referred as $\Delta A_{\text{surface}}$. Following this, the amount of water received by a system for a depth increment between z_l and z_u can be separated into ΔA_{soil} and $\Delta A_{\text{surface}}$, with an abrupt transition from ΔA_{soil} to $\Delta A_{\text{surface}}$ for even surfaces.

For uneven surfaces, ΔA_{soil} and $\Delta A_{\text{surface}}$ should be combined as a spatial average, for which Dettmann and Bechtold (2016) introduced a one-dimensional expression. The expression is briefly presented here. A microrelief can be described as a cumulative frequency distribution (F_s) of the soil surface elevations. Then, $\Delta A_{\text{surface}}$ can be calculated with

$$\Delta A_{\text{surface}} = \int_{z_l}^{z_u} F_s(z) dz \quad [2]$$

with $F_s = 1$ above the highest elevation and $F_s = 0$ below the lowest elevation.

If ΔA_{soil} and $\Delta A_{\text{surface}}$ are combined to calculate the total difference, ΔA , the soil moisture profiles must be multiplied by the fraction that is actually covered by the soil $[1 - F_s(z)]$ across the profile to obtain the spatially averaged (effective) soil moisture profiles. For a one-dimensional representation of ΔA_{soil} that accounts for microrelief effects, Eq. [1] becomes

$$\Delta A_{\text{soil}} = \int_{z_l}^{\infty} [1 - F_s(z)] [\theta(z_u - z) - \theta(z_l - z)] dz \quad [3]$$

The soil moisture profile is vertically extended above the maximum height of the surface elevation by the upper integral bound being infinity, for which the cumulative frequency distribution of the microrelief is 1 and the effective soil moisture profile is 0.

The value of ΔA is calculated by combining Eq. [2] ($\Delta A_{\text{surface}}$) and Eq. [3] (ΔA_{soil}):

$$\Delta A = \underbrace{\int_{z_l}^{z_u} F_s(z) dz}_{\Delta A_{\text{surface}}} + \underbrace{\int_{z_l}^{\infty} [1 - F_s(z)] [\theta(z_u - z) - \theta(z_l - z)] dz}_{\Delta A_{\text{soil}}} \quad [4]$$

Modeling Framework

Definition of the Soil–Vegetation Interface

In this study, we did not deal with microrelief issues but with the definition of the soil–vegetation interface at the “point” scale. For many environments, e.g., the peat moss and peat layer in

sphagnum bog ecosystems, it is hard to determine a clear position of the soil–vegetation interface due to the continuous vertical transition from soil to vegetation (indicated in Fig. 1). When placing a level staff onto the ground, a position is measured at which the penetration resistance increases to a degree that the level staff is not further penetrating into the soil. In this study, for the modeling, we looked for a position of the soil–vegetation interface that optimally separated the two water storage volumes, ΔA_{soil} and $\Delta A_{\text{surface}}$. This “optimal” position may not be consistent with the absolute level determined by the survey measurement, as for the water storage modeling the interface is best set where the strongest increase of large easily drainable macropores occurs, which commonly increase from depth to the surface (Moore et al., 2015; Morris et al., 2015). This nearly coincides with the strongest increase in S_p . Because this position is not known beforehand, the position of the interface was a parameter in the inversion. We emphasize that this parameter only adjusts the absolute level of the surface elevations, but a survey measurement is still needed for the frequency distribution of the surface elevations. We refer to the survey-measured mean surface elevation with parameter μ , which is defined to be zero in all model applications. Parameter $\Delta\mu$ (indicated in Fig. 1) is the optimized position of the interface of ΔA_{soil} and $\Delta A_{\text{surface}}$ relative to μ ($z = 0$), i.e., $\Delta\mu$ is negative when the soil–vegetation interface is lower than the survey elevation. Parameter $\Delta\mu$ can be included in Eq. [2] to [4] by substituting $F_s(z)$ with $F_s(z - \Delta\mu)$. Note that, for clarity, all given and shown water table depths here are relative to μ . Parameter $\Delta\mu$ is given as an additional parameter.

Soil Water Retention Function

We described the soil WRC by the frequently used parameterization of van Genuchten (vG) (van Genuchten, 1980):

$$\theta(h) = \begin{cases} \theta_r + \frac{\theta_s - \theta_r}{\left[1 + (|\alpha h|)^n\right]^m} & \text{for } h \leq 0 \text{ cm} \\ \theta_s & \text{for } h > 0 \text{ cm} \end{cases} \quad [5]$$

where $\theta(h)$ is the volumetric water content at pressure head h ; θ_s and θ_r ($\text{cm}^3 \text{ cm}^{-3}$) are the saturated and residual water content; and α (cm^{-1}), n (dimensionless), and m (dimensionless) are empirical parameters with $m = 1 - 1/n$. The soil was approximated as a homogeneous one-layer system.

The vG model was chosen because Dettmann et al. (2014) already investigated the sphagnum peat of our study site with laboratory evaporation experiments and inverse optimization. The results showed that the vG model was suitable to describe the peat soil moisture dynamics under laboratory conditions.

Inversion Scheme

We optimized the effective vG parameters n and α and the difference $\theta_s - \theta_r$ for a one-layer soil system. Because our approach relies only on the interpretation of water storage changes, it is

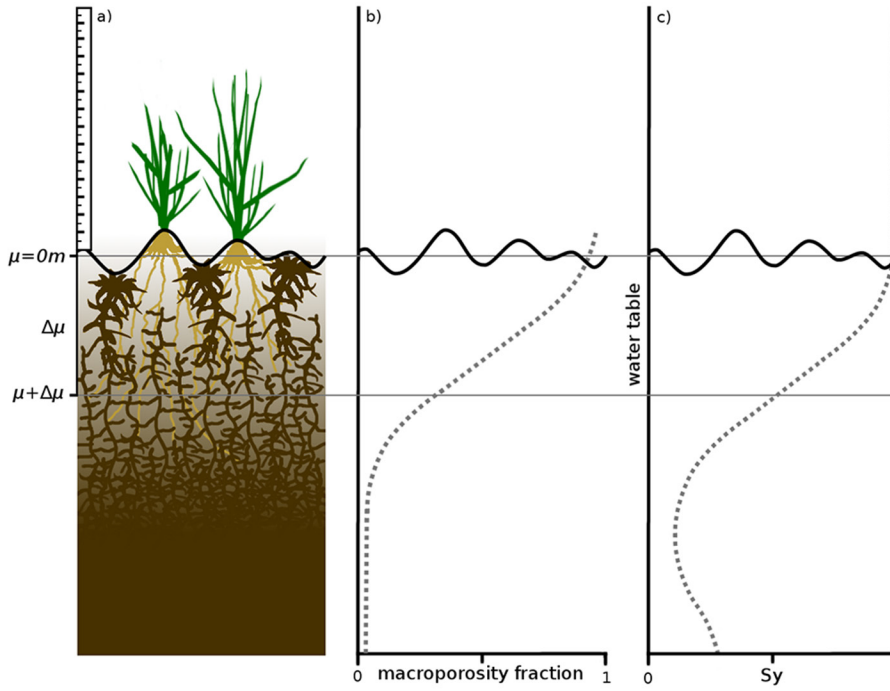


Fig. 1. Schematic illustration of the soil–vegetation transition. It is focused on the vertical soil heterogeneity and therefore microrelief is only gently indicated: (a) example sphagnum soil profile and increasing pore sizes from bottom to top, with mean surface elevation (μ) and the optimized transition between surface storage and soil ($\mu + \Delta\mu$); (b) increasing macroporosity from bottom to top; and (c) the influence of surface storage on the specific yield (S_y).

only possible to derive the difference between θ_s and θ_r and not each parameter independently. During inversion, the optimized parameters are stored in $\mathbf{x}_1 = [n, \alpha, \theta_s - \theta_r]$ and the position of the soil–vegetation interface in $\mathbf{x}_2 = [\Delta\mu]$. The observed zu ($\mathbf{zu}_{\text{obs}} = [zu_{\text{obs},1}, \dots, zu_{\text{obs},N}]$) are compared with the simulated zu ($\mathbf{zu}_{\text{sim}} = [zu_{\text{sim},1}, \dots, zu_{\text{sim},N}]$) using

$$\varepsilon_i(\mathbf{x}_1, \mathbf{x}_2) = \mathbf{zu}_{\text{obs},i} - \mathbf{zu}_{\text{sim},i}(\mathbf{x}_1, \mathbf{x}_2) \quad \text{for } i = 1, \dots, N \quad [6]$$

where N is the number of observations.

For the calculation of \mathbf{zu}_{sim} , Eq. [5] was substituted into Eq. [4]. According to the theory presented above, the resulting term was set equal the amount of P :

$$\int_{z_l}^{\infty} [1 - F_s(z - \Delta\mu)] \times \left[\frac{\theta_s - \theta_r}{\left\{1 + \left[|\alpha(zu_{\text{sim}} - z)|\right]^n\right\}^m} - \frac{\theta_s - \theta_r}{\left\{1 + \left[|\alpha(z_l - z)|\right]^n\right\}^m} \right] dz \quad [7]$$

$$+ \int_{z_l}^{zu_{\text{sim}}} F_s(z - \Delta\mu) = P$$

Because Eq. [7] cannot be solved algebraically for \mathbf{zu}_{sim} , the value was determined numerically. The cumulative frequency distribution of the soil surface elevations $F_s(z)$ was described by a normal-like (Gaussian-like) distribution.

Optimization Routine

For global optimization, we used the Markov chain Monte Carlo algorithm Differential Evolution Adaptive Metropolis (DREAM) (Vrugt et al., 2008, 2009a, 2009b). The algorithm evolves a posterior density function (pdf) of individual parameters that are treated as probabilistic variables considering the observed data set. Starting with an initial population within the feasible parameter space (prior distribution), the pdfs are evolved in multiple individual Markov chains combining the prior distribution and the data likelihood. Further information about the algorithm can be found in various publications (Vrugt et al., 2008, 2009a, 2009b; Vrugt and Ter Braak, 2011) and is not repeated here.

Following this, the parameters in \mathbf{x}_1 and \mathbf{x}_2 were derived as probabilistic distributions, resulting in an ensemble of parameter characterizations that are each consistent with the observed data. For this case, the aggregated $\varepsilon(\mathbf{x}_1, \mathbf{x}_2)$ criterion is called the *likelihood*. Details were provided by Box and Tiao (1992)

and Scharnagl et al. (2015) and are not repeated here. We used a reduced likelihood function as suggested by Scharnagl et al. (2011), where the standard derivation of $\varepsilon(\mathbf{x}_1, \mathbf{x}_2)$ is eliminated:

$$p(\tilde{y} | \mathbf{x}_1, \mathbf{x}_2) \propto \left[\sum_{i=1}^N \varepsilon_i(\mathbf{x}_1, \mathbf{x}_2)^2 \right]^{-N/2} \quad [8]$$

Model Configuration

For all model applications, the prior distributions of the vG parameters were set as a uniform distribution limited by lower and upper parameter boundaries that cover most soil types including peat (Table 1). The upper boundary of $\theta_s - \theta_r$ was constrained a little more to a value of 0.9, which is lower than reported values for sphagnum peat (0.97; Paavilainen and Päivänen, 1995). The value of 0.9 relies on θ_s values determined by Dettmann et al. (2014) near the central monitoring well and allowed a consistent comparison of the field-derived with the laboratory-derived retention curve

Table 1. Upper and lower parameter bounds of the van Genuchten parameters ($\theta_s - \theta_r$, α , and n) and the shift ($\Delta\mu$) in the measured mean surface elevation (μ) of the microrelief.

Parameter	Lower bound	Upper bound
$\theta_s - \theta_r, \text{cm}^3 \text{cm}^{-3}$	0.5	0.9
α, cm^{-1}	0.001	0.5
n	1.01	30
$\Delta\mu, \text{cm}$	−20	20

from this study, i.e., both retention curves start at a value of 0.9 and could not fall below $\theta < 0$. Due to the spatial heterogeneity around a monitoring well and within the whole study site, θ_s could differ from the determined value. However, we expected differences in θ_s to be small among the three monitoring wells because, in general, the observed differences in peat decomposition were rather small. Furthermore, laboratory-determined values of θ_s are commonly higher than θ_s values that are reached under field conditions due to wetting by capillary rise compared with wetting by precipitation, which commonly results in a higher fraction of entrapped air. Thus, we think that 0.9 is justifiable as the upper boundary of $\theta_s - \theta_r$ for the field conditions of our site.

The standard deviation (σ) of the normal distribution $F_s(z)$ of the surface elevations was set a priori individually for the three monitoring wells according to the values listed in Table 2. These values relied on the survey data.

DREAM was run with the standard configuration, evolving four parallel chains. The uniform prior distribution was sampled using Latin hypercube sampling. As convergence criteria, the Gelman and Rubin (1992) \hat{R} convergence diagnostic was set to $\hat{R} < 1.1$. After the target distribution achieved convergence, DREAM was run for 50,000 additional function evaluations to generate the pdf.

Model Application

Study Site

We applied our approach to continuous water table time series from three monitoring wells (south, central, and north) located in a near-natural ombrotrophic bog field site (Schechenfilz, 47°48' N, 11°19' E, Germany). All monitoring wells were located at the plateau of the raised bog. The bog has a 5- to 6-m-thick peat layer mainly under permanently water-saturated conditions. The peat substrate and current vegetation is dominated by sphagnum mosses, with spatially variable contributions of sedges, heather meadows, and bog pines (Hommeltenberg et al., 2014). Vegetation around the south monitoring well is only sphagnum moss. The central monitoring well is surrounded by a combination of sphagnum mosses, sedges, heather meadows, and bog pines. The vegetation composition around the north monitoring well is similar to that of the central monitoring well, except the bog pines are missing.

Table 2. Mean and lowest water tables and standard deviation (σ) of the ‘normal-like’ distributed microrelief around the three investigated monitoring wells.

Monitoring well	Mean water table	Lowest water table	σ
	—m—		
South	−0.15	−0.44	0.071
Central	−0.18	−0.44	0.089
North	−0.04	−0.32	0.061

The northern part of the bog was partly affected by peat cutting until the 1950s (Hommeltenberg et al., 2014). Because the peat cutting occurred only in parts, the peat layer is spatially variable, showing different stages of decomposition. However, in most parts the bog is still rather pristine. The peat near the central monitoring well was classified with H2 (0–0.02 m), H1 (0.02–0.12 m), and H7 (0.12–1.1 m) on the von Post scale (Drösler et al., 2015), which classifies the degree of peat humification based on the proportion of visible plant remains and the soil water color (von Post and Granlund, 1926). At the north and south monitoring wells, the soil profiles have not been classified with the von Post scale. Around the north monitoring well, relict and refilled ditches can be observed on satellite pictures. Slightly higher degrees of decomposition cannot be excluded around this monitoring well. The south of the bog complex was not affected by ditch drainage, and the sphagnum peat around the south monitoring well is pristine.

Water Tables

Water tables of all three monitoring wells are close to the surface most of the year, with a mean water table for the available time series (15 Sept. 2010–11 Nov. 2014) of −0.15 m (south monitoring well), −0.18 m (central monitoring well), and −0.04 m (north monitoring well). The minimum water tables are −0.44 m (south and central monitoring wells) and −0.32 m (north monitoring well) (see also Table 2). In our analysis, we used water table rises from z_l to z_u as a response to P in the following referred as events, with $\Delta z > 0.02$ m, $z_u < 0$ m, mean slope of the rise > 0.004 m h^{−1}, and a total sum of $P > 2$ mm.

Microrelief

The Schechenfilz bog complex has a considerable microrelief consisting of hummocks and hollows (Nungesser, 2003). Because water table changes are affected by the microrelief, the surface elevation was measured around the three investigated monitoring wells. Along six 8-m transects, each beginning at the monitoring well, elevations were measured every 0.25 m in relation to the elevation of the monitoring well. However, as detailed above, sphagnum bogs are characterized by a continuous transition from peat soil to vegetation (Fig. 1), and it is hardly possible to define and measure a soil–vegetation interface. Thus, to obtain objective and reproducible elevation data, we placed a level staff (locating surface: 17 cm²; weight: 1.8 kg) onto the ground without manually adding any extra pressure.

Figure 2 shows the surface elevation distributions as an example around the south monitoring well and the fitted normal frequency distribution and F_s used in the inversion. Usually water table depths are determined with respect to the surface height at the location of the monitoring well. However, this makes water table depths dependent on the specific microtopographic position of the monitoring well, and the comparison of water table depths with other monitoring wells in the study site is often more influenced by this arbitrary position and less by real differences in hydrology.

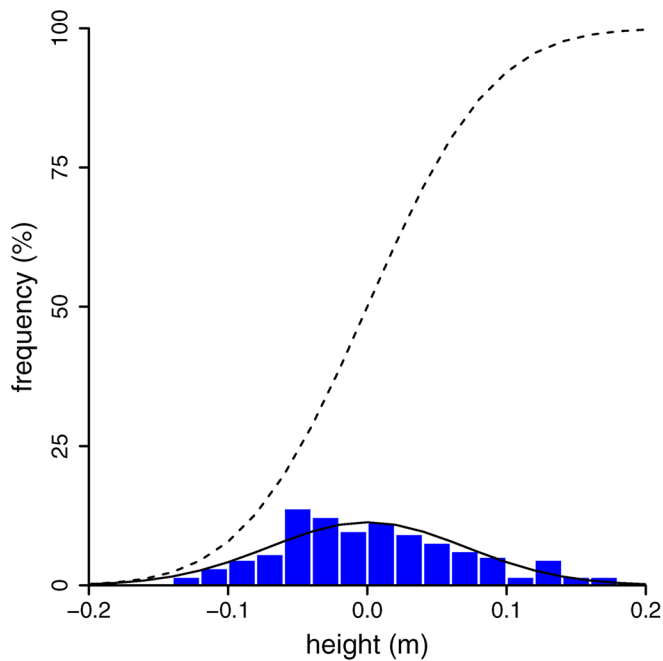


Fig. 2. Measured (blue bars) and fitted surface elevation distribution (black solid line) and fitted cumulative surface elevation distribution (F_s) (black dashed line) of all six measured transects around the south monitoring well. Measured heights are relative to the mean surface elevation μ at $z = 0$.

Therefore, in this study, all water tables were related to the mean surface elevation (μ) of zero for the area around the monitoring well.

Frequency distributions of surface elevations were similar and “normal-like” around all three monitoring wells. Table 2 gives the standard deviations (σ) of the fitted normal distributions for the south, central, and north monitoring wells.

Results and Discussion

Event Detection and Prediction of Water Table Rises

The predefined criteria were fulfilled for 145 events for the south monitoring well, 113 events for the central well, and 114 events for the north well. Differences in the number of detected events among the monitoring wells were caused by differences in the values of Δz , z_u , and the mean slope of the water table rise.

Figure 3a illustrates, as in Fig. 2 also for the south monitoring well, the water table rises from z_l to z_u vs. S_y , calculated from the detected events ($S_y = \Delta z/P$; Logsdon et al., 2010). Most of the detected events were close to the surface. As seen in Fig. 3a, S_y values increased for near-surface water table rises. This clearly indicates the contribution of the surface storage for shallow water tables and demonstrates the necessity of accounting for the micro-relief when predicting shallow water table changes. For lower water tables, the influence of the WRC of the soil increased.

Figure 3a further indicates that a macroporous layer (with high S_y values) below the measured mean surface elevation contributed to the surface storage (see also above). This can be seen by the S_y values for the events with water tables between approximately -0.2 and -0.1 m. Applying the normally distributed surface elevations of the microrelief ($\sigma = 0.071$ m, $\mu = 0$) at the south monitoring well to a water table change from -0.2 to -0.1 m results into a $S_{y,\text{surface}}$ value of 0.02504 (after division by Δz). Thus, the S_y values shown in Fig. 3a have an offset to the expected behavior of about 0.10 m. This offset can be explained by a topsoil layer that acts like a porous system that releases water in the range of the occurring matrix potential fluctuations. How deep the top surface soil acts like surface storage is shown by the optimization of $\Delta\mu$ as detailed above. The water table rises from z_l to z_u vs. S_y at the central monitoring well (not shown) showed a similar behavior as at the south monitoring well. At the north monitoring well (not shown), the water table rises vs. S_y indicated a lower contribution of the top surface soil to the surface storage.

For all three investigated monitoring wells, the 95% confidence intervals (CI_{95}) of the simulated water table changes, obtained from the pdfs, matched the observed ones fairly accurately for both deep and shallow water tables (Fig. 3b; again only shown as an example for the south monitoring well).

Posterior Density Functions and Water Retention Characteristics

Posterior Density Functions

The pdfs of the estimated vG parameters and $\Delta\mu$ are depicted in Fig. 4 for the south and central monitoring wells (horizontal axes for parameters α , n , and $\Delta\mu$ are narrowed from the uniform prior). The corresponding CI_{95} quantiles of the optimized parameters n , α , and $\Delta\mu$ are given in Table 3 for all three monitoring wells.

In proportion to the prior distribution of n (1.01–30), α (0.001–0.5 cm^{-1}), and $\Delta\mu$ (–20 to 20 cm), the pdfs of the south and central monitoring wells are well constrained. In contrast, the results for the north monitoring well demonstrate the applicability limits of our approach. For the north monitoring well, the inversion failed to constrain parameter n at the lower boundary of the prior distribution, and the pdf of parameter α is wide compared with the south and central monitoring wells. This leads to unrealistic soil WRC within the CI_{95} . We interpret this as a failure of our approach for the north monitoring well. Water tables at the north monitoring well are approximately 0.1 m shallower than at the other monitoring wells. For the south and central monitoring wells, S_y values increased for events with $z_l < -0.3$ m, reaching S_y values of approximately 0.2 (indicated in Fig. 3a for the south monitoring well). The increasing S_y values at comparatively low water tables indicate that the soil substantially releases water at equivalent pressure heads in the upper soil. For constraining the vG parameters α and n , this information is crucial because these parameters define at which pressure heads the soil dewater substantially and

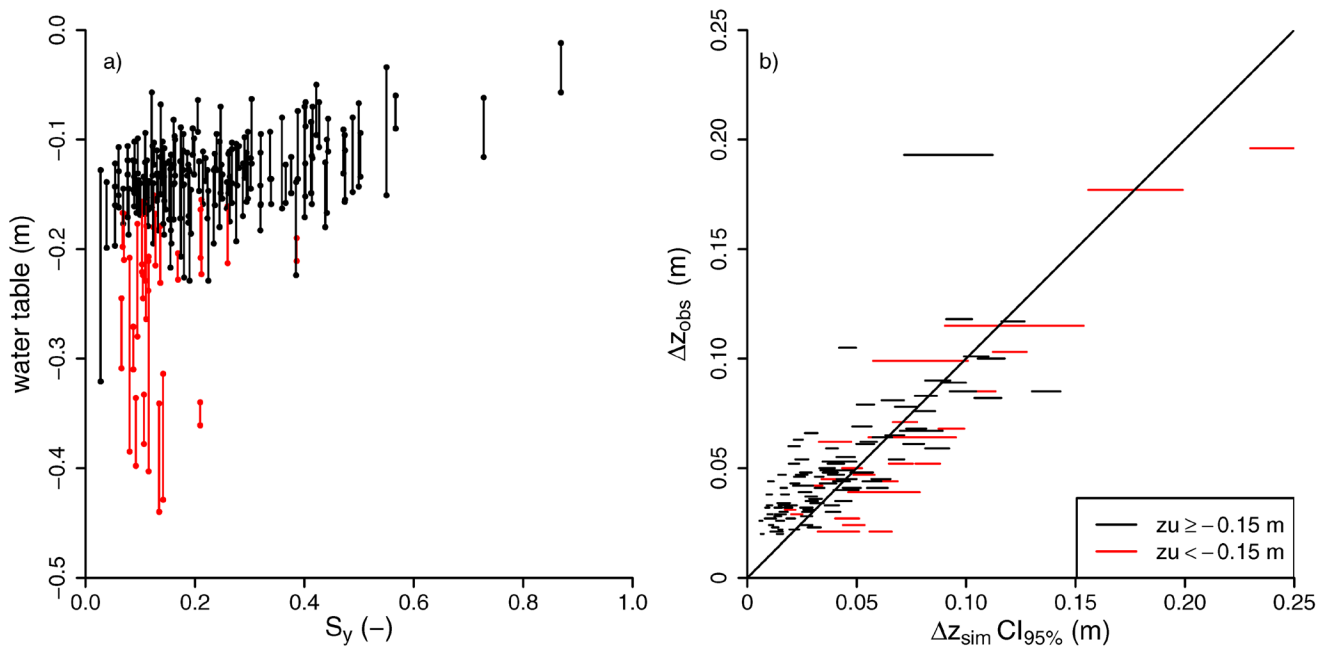


Fig. 3. (a) Water table rise (from a lower level at z_l to an upper level at z_u) vs. the specific yield (S_y) of the detected events at the south monitoring well. The value of S_y was calculated for each event ($S_y = \Delta z/P$, where P is the precipitation); and (b) observed water table changes (Δz_{obs}) vs. 95% confidence intervals (CI_{95}) of simulated water table changes (Δz_{sim}) for the south monitoring well. The red lines represent Δz with $z_u < -0.15$ m; the black lines are Δz with $z_u \geq -0.15$ m.

how abruptly this occurs. The lowest water table in the time series for the north monitoring well was -0.32 m. Below -0.3 m, three events were detected with S_y values between 0.07 and 0.08. However, these S_y values are not increased compared with events at shallower water tables. Following this, at the north monitoring well, the deepest water tables were not sufficient, i.e., the extent of the unsaturated zone was too limited, so that a substantial dewatering of the topsoil did not take place. Therefore, the vG parameters n and α could not be constrained.

For all monitoring wells, the inversion failed to constrain $\theta_s - \theta_r$. The information for the lowest water tables was not sufficient to constrain $\theta_s - \theta_r$.

Differences between South and Central Monitoring Wells

The uncertainty bounds (CI_{95}) of the optimized soil WRC are visualized in Fig. 5. Also depicted is one of the soil WRC derived by Dettmann et al. (2014) near the central monitoring well. The figure shows a steeper decline of the soil WRC for decreasing pressure heads (increasing suctions) for the south monitoring well than for the central monitoring well. This indicates that the peat at the south monitoring well has a narrower pore size distribution (higher vG parameter n) and thus dewateres more abruptly. This may be an effect of different peat degradation and plant composition of the peat substrates, with pure sphagnum at the south monitoring well and the combination of sphagnum, sedges, heather meadows, and bog pines at the central monitoring well. According to Bartels and Kuntze (1968), pristine sphagnum peat is characterized by

a more abrupt dewatering characteristic than less pristine sphagnum peat. In former centuries, the central monitoring well was probably partly affected by nearby ditch drainage. Hence the peat around the south monitoring well was expected to be more pristine, although this was not determined directly at the site. Following this, the steeper soil WRC at the south monitoring well (shown in Fig. 5) may be related to the more pristine peat than at the central monitoring well. The pressure heads at which the soils start to dewater substantially are in the same range for both monitoring wells, which is indicated by only slight differences in the characteristic pore size ($1/\alpha$).

There are also methodological errors that may have contributed to the differences in parameters between the monitoring wells. They are discussed below.

Comparison between Field and Laboratory

Dettmann et al. (2014) studied the WRC of the sphagnum peat at the study site near the central monitoring well with evaporation experiments and inverse optimization. Laboratory values from their study ($\alpha = 0.0456 \text{ cm}^{-1}$, $n = 1.72$) indicate an earlier (at lower suctions) dewatering compared with the WRC determined in situ (Fig. 5). This difference between the WRC indicates that WRC determined in the laboratory may not be transferrable to the field. To investigate the transferability, we predicted water table changes with Eq. [7] by applying the laboratory WRC and the surface storage parameters, i.e., σ from the survey data and $\Delta\mu$ of the optimization (median of the pdf). Figure 6 shows the observed water table changes for the central monitoring well plotted vs. the

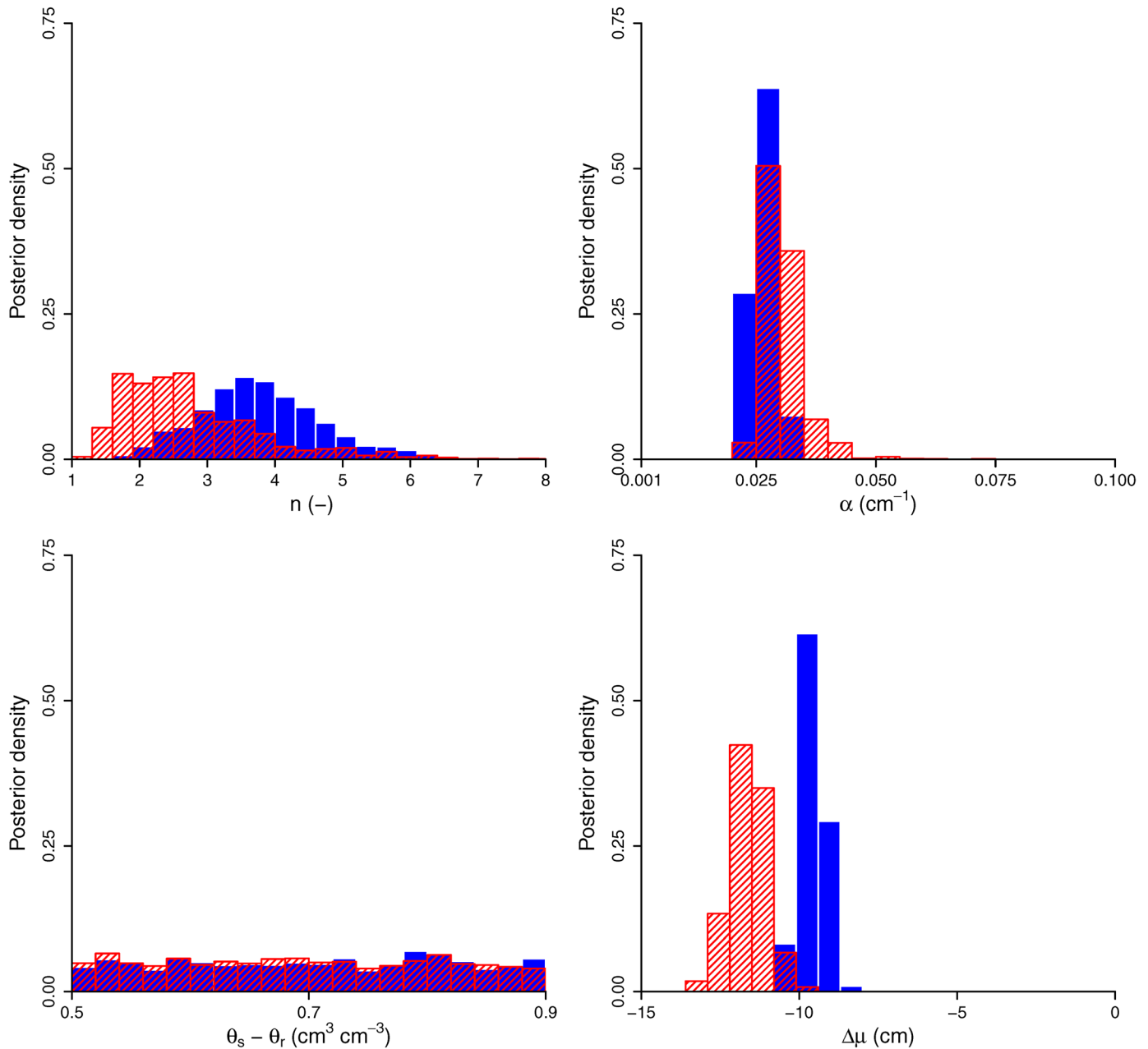


Fig. 4. Posterior density functions (pdfs) of the optimized van Genuchten (vG) parameters n , α , and $\theta_s - \theta_r$ and the optimized shift ($\Delta\mu$) to the measured mean surface elevation (μ) of the microrelief. The pdfs of the central monitoring well are in red, while the pdfs of the south monitoring well are in blue.

predicted values. The figure indicates a bias of the prediction toward underestimated water table changes.

Besides methodological errors (discussed below) that may influence the parameters derived in situ, it can be speculated about different hydraulic behavior of the peat under laboratory and field conditions. As mentioned above, shrinkage and swelling of peat might be more distinctive under laboratory conditions. This affects the θ - h relation derived in the laboratory. Note that we defined the reference volume to calculate the volumetric moisture, θ , to be constant (cracks still belong to the total peat volume). It is

known that shrinkage, as a result of increasing soil water suction, partly releases water stresses (Baumgartl and Köck, 2004), i.e., in the laboratory more water is effectively released at low suctions. In other words, with the laboratory WRC, more water can be stored in the unsaturated peat profile when it rains, i.e., the predicted water table changes underestimate the observed changes.

A second reason for the underestimation of the water table changes might be a scale effect. In the laboratory, the soil samples had a height of 0.2 m and width of 0.3 m. They were taken from the upper part of the peat profile, just below the vegetation layer. In

Table 3. Lower and upper bounds of the 95% confidence intervals (CI_{95}) of the posterior density functions (pdf) from the optimized van Genuchten parameters n and α and the shift ($\Delta\mu$) to the measured mean surface elevation (μ) of the microrelief.

Monitoring well	n	α	$\Delta\mu$
		cm^{-1}	cm
South	2.17–6.04	0.022–0.031	–10.3 to –8.9
Central	1.46–5.78	0.025–0.042	–12.7 to –10.4
North	1.09–3.21	0.020–0.119	–2.2 to –0.1

contrast, the in situ WRC represents a spatial integration around the monitoring well while assuming a uniform soil profile with a vertical extent of about 0.65 m, which is the distance between the highest surface elevation and the lowest water table of the time series. As for rather pristine peatlands, where porosity and pore sizes commonly decrease with depth, the observed water table changes are higher than the ones predicted from laboratory parameters that were only based on samples of the upper 0.2 m of the peat profile.

Transition between Soil and Surface Storage

The CI_{95} of the derived pdfs of $\Delta\mu$ (Fig. 4) are between –8.9 and –10.4 cm for the south monitoring well, between –10.4 and –12.7 cm for the central monitoring well, and between –2.2 and –0.1 cm for the north monitoring well (also listed in Table 3). Regarding the south monitoring well, the pdf of $\Delta\mu$ confirms the visual assumption from Fig. 3a that approximately the top 0.1 m of the soil contains a high amount of macropores, i.e., presents high

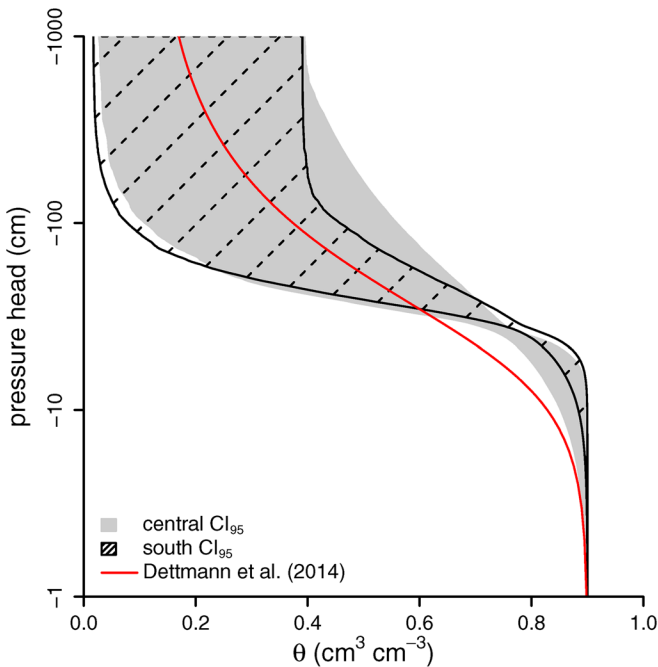


Fig. 5. Soil water retention characteristics (WRC) 95% confidence intervals (CI_{95}) for the south and central monitoring wells and soil WRC of Dettmann et al. (2014) near the central monitoring well.

S_y values and thus is better described by $\Delta A_{\text{surface}}$. The same effect was observed for the central monitoring well.

Discussion of Uncertainties

Uncertainties of Input Variables

Figure 3a shows that there is considerable scatter in the depth dependency of S_y obtained from the analyzed rain events and related water table rises. This scatter can be attributed to several potential error sources, which can be separated into precipitation- and soil-related errors and can be both statistical and systematic.

About 35% of the P events were measured with a gauge within the bog, 30 to 325 m away from the three monitoring wells. Given the proximity, the error due to spatial variability of P can be considered low for these data. However, data gaps were filled with data from the German weather forecast station Eberfing, which is 10 km away. The spatial variability of P can be high for such distances. Further, the distance leads to a temporal offset of the rainfall. For the gap-filled data, thus, we expect higher errors for the total P sums of the events. Comparing the P sums of the two rain gauges for the overlap period did not show any systematic difference. The P sums were either higher or lower for the same event. This can be an effect of different wind directions, wind speeds, or other climate conditions. Given the short overlap period, a correction of the error by the distant rain gauge was not possible.

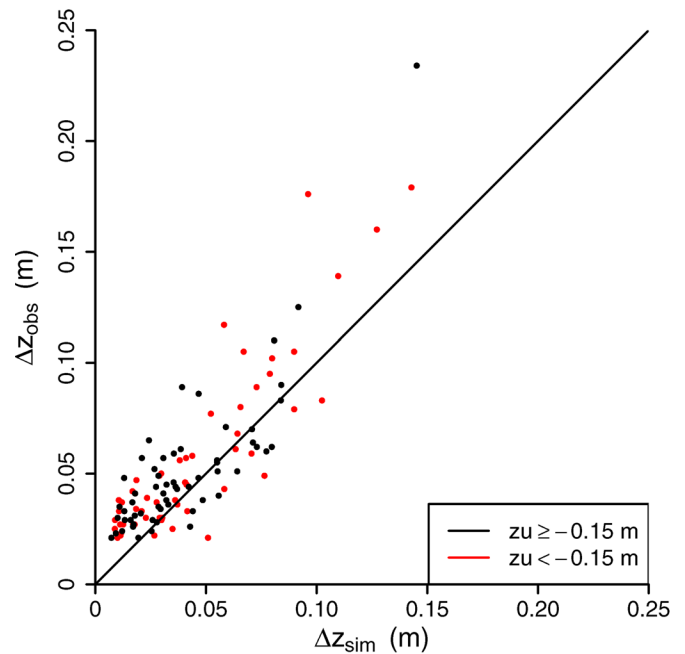


Fig. 6. Observed water table changes (Δz_{obs}) at the central monitoring well vs. simulated water table changes (Δz_{sim}) calculated with the WRC by Dettmann et al. (2014) near the central monitoring well. The red points represent deeper Δz with upper water table depth $z_u < -0.15$ m and the black points are shallower Δz with $z_u \geq -0.15$ m.

Measurements with P gauges are adversely affected by undercatch bias, induced by wind turbulence, evaporative losses, wetting losses, or mechanical plugging (Groisman and Legates, 1994). The P undercatch is highly variable depending on the wind characteristic (Neff, 1977). On average, measured P values are lower than the actual P . In contrast, measured P values are higher than the amount of water that actually infiltrated due to interception in the vegetation layer. Regarding Δz , several model assumptions for the soil processes are not entirely fulfilled in reality. Macropore flow, lateral flow, shrinkage and swelling, hydraulic gradients within the soil profile before and after P , and water repellency effects are variable in their presence and intensity among the different events and thus lead to statistical and systematic errors.

The pore size distribution of the peat soil matrix and surface elevations change due to shrinkage and swelling. Therefore, hydraulic properties can be different for different P events. This can affect the corresponding Δz and contributes to the scatter in Fig. 3.

During macropore flow, water is bypassing the soil matrix (Dekker and Ritsema, 1996). At our site, such flow might be channeled through root channels and along coarse peat-forming plant material. As result, water tables rise abruptly, with a successive decline after the maximum when water redistributes into the soil matrix. We observed immediate and steep water table declines directly after the water table maximum for a variety of events for both deep and shallow water table rises but not for all. When water tables showed such a decline, the length and steepness of the decline was very variable. This shows that macropore flow is variable and the intensity may depend on several conditions, such as, e.g., the P intensity or water repellency condition of the sphagnum moss and peat before P . Water repellency is a time-dependent physical property of the soil (Dekker and Ritsema, 1996). It depends on the initial moisture at an event and can induce macropore flow. In dependence on the degree of decomposition and plant origin, sphagnum mosses and peats have been reported to be either water repellent (Michel et al., 2001) or hydrophilic (Kettridge et al., 2014). For the investigated study site, no water repellency measurements have been done. It is possible that water repellency conditions occur in the top centimeters for deep water tables during dry periods. Because the decline behavior after water table rises was very variable and for longer time periods and lateral water fluxes may become important, we decided not to correct Δz for the decline. Thus, if macropore flow and water repellency are relevant for our site, the measured Δz values are systematically higher than the prediction of a model that ignores these processes.

Further, deviations from the hydrostatic equilibrium assumption within the soil profile before and after P and lateral fluxes during the event may generate further uncertainty. If drying-induced deviations from hydrostatic equilibrium within the soil profile occurred due to an evapotranspiration period before the event, parts of P would wet up the soil instead of causing Δz . Deviations

from hydrostatic equilibrium have been observed for peatlands, e.g., by Lukenbach et al. (2016), during extended periods without rainfall and for water levels lower than -0.6 m in the Utikuma Lake Research Study Area of the Boreal Plain ecozone. However, at our site we expected the soil moisture profile to be close to hydrostatic equilibrium before and after P events, as pressure observations from unpublished tensiometer data at -10 -, -20 -, and -30 -cm depths showed for this peat soil. For the top vegetation–soil layer, however, deviations from hydrostatic equilibrium may occur due to evapotranspiration. Furthermore, it should be noted that in peatlands with less humid climates and deeper water tables, deviations from hydrostatic equilibrium may be higher for the whole profile.

A water storage change due to the local difference in lateral in- and outflow (i.e., local flow divergence) represents another error source. In particular, for shallower water tables, overland flow directed out of the bog system may occur during the time span of the event and generate significant local differences of lateral in- and outflows within the peatland. We emphasize that we do not refer here to the magnitude of the lateral fluxes, which can be very high during precipitation events, but to the local differences in them that generate water storage changes. These lateral flux differences are neglected in our approach for the time period of an event. Both vertical hydraulic gradients during evapotranspiration periods and lateral fluxes lead to measured Δz values that are systematically lower than the prediction of a model that neglects these influences. It can be noted that for both input variables, P and Δz , there are statistical errors and opposing systematic errors. Because sufficient information about the error sources is not available for a reliable quantification, our strategy in this study was to not attempt to correct for any bias and to apply the data as they are.

Influence of Uncertainties on Obtained Water Retention Characteristics

Above, we discussed the differences between the obtained soil WRC at the south and central monitoring wells and how they could be explained by field variability. From the uncertainty discussion here, it becomes obvious that also methodological errors that deviate among the monitoring wells may have contributed to these differences. The observed water table rises at the south and central monitoring wells showed different Δz for the same P events. For most events, Δz was higher at the south monitoring well than at the central monitoring well. This led to different n and $\Delta \mu$ values at the south monitoring well.

Most of the error sources above may have led to higher Δz at the south monitoring well compared with the central monitoring well. The most evident influence may have had the different compositions of the vegetation at the two monitoring wells. At the central monitoring well, a combination of sphagnum mosses, sedges, heather meadows, and bog pines is present, while the south monitoring well is surrounded by sphagnum mosses only. We expect

substantially higher interception for the higher vegetation at the central monitoring well, which would directly decrease Δz because less water would have actually infiltrated.

Further, one could argue that water repellency and macropore flow are more relevant at the south compared with the central monitoring well. The lower vegetation at the south monitoring well may have led to an enhanced drying of the uppermost soil-vegetation layer, which may have provoked flow channeling due to water repellency and thus macropore flow. In contrast, higher vegetation at the central monitoring well additionally decreased the rainfall intensity due to the retardation effect of the canopy, which further increased the potential macropore flow at the south compared with the central monitoring wells.

Summarizing, both statistical and systematic uncertainties influence the shape and scatter of the observed depth distribution of S_y (indicated in Fig. 3a). The obtained pdfs are less constrained and potentially biased due to these uncertainties. Systematic uncertainties can have a different extent at different monitoring wells and therefore may result in apparently different soil WRC within a study site. The magnitude of these uncertainties relative to the actual field variability was beyond the scope of this study.

Benefit of the New Approach

We have provided a new approach for the determination of the effective soil WRC, obtained in situ in the natural environment and as a spatial average around a monitoring well. The proposed approach requires only water table and P measurements, and for field sites with uneven surfaces, additional information about the surface elevation distribution of the microrelief around the monitoring well. Therefore, labor-intensive determination in the laboratory on small soil samples and the typical uncertainties of such methods (e.g., compaction or disturbance of the soil structure) can be avoided. Furthermore, the soil WRC of our approach are obtained for more representative soil volumes compared with laboratory soil samples. A disadvantage of our approach is that time series of a few years are required to obtain sufficient events that can be analyzed.

As an application example, we want to highlight the relevance of our study to improve the methodology of an evapotranspiration estimation approach. Evapotranspiration is frequently estimated by water table depth fluctuations following the method of White (1932) (Fahle and Dietrich, 2014; Loheide et al., 2005; McLaughlin and Cohen, 2014; Mould et al., 2010; Wang and Pozdniakov, 2014). The method of White (1932) uses diurnal patterns consisting of a water table decline in the daytime and a recovery phase overnight. Following the theory of White (1932) and above, evapotranspiration can be calculated directly with Eq. [4] for shallow water table changes if knowledge about the soil WRC is available. Using the soil WRC obtained by the approach of this study improves the estimation substantially. First, the soil

WRC are directly estimated at the monitoring well, and the vG parameters are available as pdfs. Thus, uncertainties can be propagated to the evapotranspiration estimates. In our opinion, this is essential because evaporation estimates usually are highly uncertain. Second, surface storage plays a major role in the estimation at shallow groundwater systems. However, if the top vegetation at the soil surface contributes to the surface storage, as is shown by the optimization of $\Delta\mu$, surface storage is substantially underestimated. The optimization of $\Delta\mu$ gives the possibility for a better estimation of the surface storage. This leads to more realistic evapotranspiration estimates.

Further, the optimization of $\Delta\mu$ can substantially contribute to research on the microrelief of shallow groundwater systems. For these systems, a separation into vegetation and soil layer is often difficult. The particular height of this interface cannot be defined objectively, regardless whether data are derived by surveying or by laser scanning. The optimization of $\Delta\mu$ gives an objective estimation about the depth of the soil-vegetation interface from a hydrological perspective.

Summary and Conclusions

The in situ determination of soil hydraulic properties by inverse modeling of field observations is difficult for peatlands when trying to use the full time series because there are large uncertainties in lateral flow and evapotranspiration. In this study, we thus focused only on the periods of water table rises caused by P . Our study indicated that these observations can contain sufficient information to constrain the wet range of the soil WRC around monitoring wells in peatlands. For two of the three investigated monitoring wells, the obtained soil WRC are in a plausible range and comparable to soil WRC determined in the laboratory for the site and to those of previous studies for similar sites (Bartels and Kuntze, 1968; Dettmann et al., 2014; Letts et al., 2000; Price et al., 2008). At one monitoring well, water tables were not low enough and the upper soil did not dewater enough to derive information about the soil WRC. In principle, our approach should also be applicable to other shallow groundwater systems, which however needs further field evaluation.

The major advantages of our approach over laboratory methods is the determination of soil WRC at more representative scales and under typical dynamic field conditions. Other site-specific factors, as for example shrinkage and swelling, which is typical for peatlands and leads to a significant fluctuating soil surface, are lumped together in the description of the effective soil WRC obtained from our approach.

For low pressure heads (high suctions), the indicated uncertainty was high. Because most of the unsaturated zone of peat soils remains very wet throughout the year, the effective soil moisture variations occur in the wet range of the soil water retention

curve. Thus, water table depth observations do not provide the necessary information to constrain the dry range, i.e., $\theta_s - \theta_r$ could not be constrained.

Besides this inevitable limitation in the dry range, uncertainty can be reduced with high-quality and continuous P data observed directly at the field site. Further, there are several potential systematic errors due to simplified model assumptions. Given the lack of knowledge about detailed peat properties, their relevance can hardly be evaluated. Non-equilibrium phenomena such as hydrophobicity and macropore flow may be investigated by the water table declines after the maximum of the events in combination with soil moisture probes. More knowledge about such processes could help to improve the method developed in this study. A quantitative consideration was beyond the scope of this study and should be a topic of future research.

Finally, we emphasize that our approach did not account for vertical soil heterogeneity but has been used to estimate effective parameters assuming a uniform soil profile. In particular for peat soils, vertical heterogeneity often occurs and can be high (Morris et al., 2015), and functions describing typical vertical trends could be used to advance our approach.

Acknowledgments

We acknowledge the financial support by the joint research project Organic Soils funded by the Thünen Institute. We appreciate support from Bärbel Tiemeyer (Thünen Institute, Braunschweig), Enrico Frahm (PTB, Braunschweig), Eike Maurer, Annette Freibauer (LFL, Freising), Benedikt Scharnagl (UFZ, Halle), Marika Bernrieder, and Janina Hommeltenberg (KIT, Garmisch-Partenkirchen). We further thank the District Government of Upper Bavaria for making access to the site possible. Special thanks to Jan Vanderborght as associate editor for his excellent comments and suggestions to improve the manuscript. We are grateful to Martine van der Ploeg for her review that included several helpful comments and suggestions, to a second anonymous reviewer, and to Insa Neuweiler as co-editor.

References

- Ankeny, M.D., M. Ahmed, T.C. Kaspar, and R. Horton. 1991. Simple field method for determining unsaturated hydraulic conductivity. *Soil Sci. Soc. Am. J.* 55:467–470. doi:10.2136/sssaj1991.03615995005500020028x
- Bartels, R. and H. Kuntze. 1968. Ungesättigte hydraulische Leitfähigkeit von Moorböden. *Göttinger Bodenkundliche Berichte*. Vol. 1. p. 155–161
- Basile, A., G. Ciollaro, and A. Coppola. 2003. Hysteresis in soil water characteristics as a key to interpreting comparisons of laboratory and field measured hydraulic properties. *Water Resour. Res.* 39:1355. doi:10.1029/2003WR002432
- Baumgartl, Th., and B. Köck. 2004. Modeling volume change and mechanical properties with hydraulic models. *Soil Sci. Soc. Am. J.* 68:57–65. doi:10.2136/sssaj2004.5700
- Bodhinayake, W., B.C. Si, and K. Noborio. 2004. Determination of hydraulic properties in sloping landscapes from tension and double-ring infiltrometers. *Vadose Zone J.* 3:964–970. doi:10.2136/vzj2004.0964
- Box, G.E.P., and G.C. Tiao. 1992. Bayesian inference in statistical analysis. John Wiley & Sons, New York. doi:10.1002/9781118033197
- Cheng, D., Y. Wang, J. Duan, X. Chen, and S. Yang. 2015. A new analytical expression for ultimate specific yield and shallow groundwater drainage. *Hydrol. Processes* 29:1905–1911. doi:10.1002/hyp.10306
- Chow, T.L., H.W. Rees, I. Ghanem, and R. Cormier. 1992. Compactibility of cultivated sphagnum peat material and its influence on hydrologic characteristics. *Soil Sci.* 153:300–306. doi:10.1097/00010694-199204000-00006
- Dekker, L.W., and C.J. Ritsema. 1996. Variation in water content and wetting patterns in Dutch water repellent peaty clay and clayey peat soils. *Catena* 28:89–105. doi:10.1016/S0341-8162(96)00047-1
- Dettmann, U., and M. Bechtold. 2016. One-dimensional expression to calculate specific yield for shallow groundwater systems with microrelief. *Hydrol. Processes* 30:334–340. doi:10.1002/hyp.10637
- Dettmann, U., M. Bechtold, E. Frahm, and B. Tiemeyer. 2014. On the applicability of unimodal and bimodal van Genuchten–Mualem based models to peat and other organic soils under evaporation conditions. *J. Hydrol.* 515:103–115. doi:10.1016/j.jhydrol.2014.04.047
- Dimitrov, D.D., R.F. Grant, P.M. Lafleur and E.R. Humphreys. 2010. Modeling the subsurface hydrology of Mer Bleue Bog. *Soil Sci. Soc. Am. J.* 74:680–694. doi:10.2136/sssaj2009.0148
- Drösler, M., N. Roskopf, J. Hommeltenberg, J. Eberl, A. Shomnath, and H.P. Schmid. 2015. Klimarelevanz von Hochmooren am Alpenrand: Standort, Vegetation, Nutzung und Treibhausgasemissionen der ICOS-Standorte Mooseurach bei Königsdorf und Schechenfilze bei Seeshaupt. Vol. 117, Exkursionsführer. Deutschen Bodenkundlichen Gesellschaft, München.
- Durner, W., and K. Lipsius. 2005. Determining soil hydraulic properties. In: M.G. Anderson and J.J. McDonnell, editors, *Encyclopedia of hydrological sciences*. John Wiley & Sons, Chichester, UK. p. 1121–1144. doi:10.1002/0470848944
- Fahle, M., and O. Dietrich. 2014. Estimation of evapotranspiration using diurnal groundwater level fluctuations: Comparison of different approaches with groundwater lysimeter data. *Water Resour. Res.* 50:273–286. doi:10.1002/2013WR014472
- Gelman, A., and D.B. Rubin. 1992. Inference from iterative simulation using multiple sequences. *Stat. Sci.* 7:457–472. doi:10.1214/ss/1177011136
- Groisman, P.Y., and D.R. Legates. 1994. The accuracy of United States precipitation data. *Bull. Am. Meteorol. Soc.* 75:215–227. doi:10.1175/1520-0477(1994)075<0215:TAOUP>2.0.CO;2<0215:taoup>2.0.co;2
- Holden, J., P.J. Chapman, and J.C. Labadz. 2004. Artificial drainage of peatlands: Hydrological and hydrochemical process and wetland restoration. *Prog. Phys. Geogr.* 28:95–123. doi:10.1191/0309133304pp403ra
- Hommeltenberg, J., H.P. Schmid, M. Drösler, and P. Werle. 2014. Can a bog drained for forestry be a stronger carbon sink than a natural bog forest? *Biogeosciences* 11:3477–3493. doi:10.5194/bg-11-3477-2014
- Hvorslev, M.J. 1951. Time lag and soil permeability in ground-water observations. *Waterways Exp. Stn. Bull.* 36. US Army Corps Eng., Vicksburg, MS.
- Jadoon, K.Z., L. Weihermüller, B. Scharnagl, M.B. Kowalsky, M. Bechtold, S.S. Hubbard, et al. 2012. Estimation of soil hydraulic parameters in the field by integrated hydrogeophysical inversion of time-lapse ground-penetrating radar data. *Vadose Zone J.* 11(4). doi:10.2136/vzj2011.0177
- Jury, W., D. Or, Y. Pachepsky, H. Vereecken, J. Hopmans, L. Ahuja, et al. 2011. Kirkham's legacy and contemporary challenges in soil physics research. *Soil Sci. Soc. Am. J.* 75:1589–1601. doi:10.2136/sssaj2011.0115
- Kettridge, N., R.E. Humphrey, J.E. Smith, M.C. Lukenbach, K.J. Devito, R.M. Petrone, and J.M. Waddington. 2014. Burned and unburned peat water repellency: Implications for peatland evaporation following wildfire. *J. Hydrol.* 513:335–341. doi:10.1016/j.jhydrol.2014.03.019
- Lafleur, P.M., R.A. Hember, S.W. Admiral, and N.T. Roulet. 2005. Annual and seasonal variability in evapotranspiration and water table at a shrub-covered bog in southern Ontario, Canada. *Hydrol. Processes* 19:3533–3550. doi:10.1002/hyp.5842
- Letts, M.G., N.T. Roulet, N.T. Comer, M.R. Skarupa, and D.L. Versegny. 2000. Parametrization of peatland hydraulic properties for the Canadian Land Surface Scheme. *Atmos.–Ocean* 38:141–160. doi:10.1080/07055900.2000.9649643
- Logsdon, S.D., K.E. Schilling, G. Hernandez-Ramirez, J.H. Prueger, J.L. Hatfield, and T.J. Sauer. 2010. Field estimation of specific yield in a central Iowa crop field. *Hydrol. Processes* 24:1369–1377. doi:10.1002/hyp.7600
- Loheide, S.P., II, J.J. Butler, Jr., and S.M. Gorelick. 2005. Estimation of groundwater consumption by phreatophytes using diurnal water table fluctuations: A saturated–unsaturated flow assessment. *Water Resour. Res.* 41:W07030. doi:10.1029/2005WR003942
- Lukenbach, M.C., K.J. Devito, N. Kettridge, R.M. Petrone, and J.M. Waddington. 2016. Burn severity alters peatland moss water availability: Implications for post-fire recovery. *Ecohydrology* 9:341–353. doi:10.1002/eco.1639
- Mapa, R.B., R.E. Green, and L. Santo. 1986. Temporal variability of soil hydraulic properties with wetting and drying subsequent to tillage. *Soil Sci. Soc. Am. J.* 50:1133–1138. doi:10.2136/sssaj1986.03615995005000050008x
- McLaughlin, D.L., and M.J. Cohen. 2014. Ecosystem specific yield for estimating evapotranspiration and groundwater exchange from diel surface water variation. *Hydrol. Processes* 28:1495–1506. doi:10.1002/hyp.9672
- Michel, J.C., L.M. Rivière, and M.N. Bellon-Fontaine. 2001. Measurement of the wettability of organic materials in relation to water

- content by the capillary rise method. *Eur. J. Soil Sci.* 52:459–467. doi:10.1046/j.1365-2389.2001.00392.x
- Mitchell, A.R. 1991. Soil surface shrinkage to estimate profile soil water. *Irrig. Sci.* 12:1–6. doi:10.1007/BF00190702
- Mitchell, A.R., and M.Th. van Genuchten. 1992. Shrinkage of bare and cultivated soil. *Soil Sci. Soc. Am. J.* 56:1036–1042. doi:10.2136/sssaj1992.03615995005600040006x
- Moore, P.A., P.J. Morris, and J.M. Waddington. 2015. Multi-decadal water table manipulation alters peatland hydraulic structure and moisture retention. *Hydrol. Processes* 29:2970–2982. doi:10.1002/hyp.10416
- Morris, P.J., A.J. Baird, and L.R. Belyea. 2015. Bridging the gap between models and measurements of peat hydraulic conductivity. *Water Resour. Res.* 51:5353–5364. doi:10.1002/2015WR017264
- Mortl, A., R. Muñoz-Carpena, D. Kaplan, and Y. Li. 2011. Calibration of a combined dielectric probe for soil moisture and porewater salinity measurement in organic and mineral coastal wetland soils. *Geoderma* 161:50–62. doi:10.1016/j.geoderma.2010.12.007
- Mould, D.J., E. Frahm, T. Salzmann, K. Miegel, and M.C. Acreman. 2010. Evaluating the use of diurnal groundwater fluctuations for estimating evapotranspiration in wetland environments: Case studies in southeast England and northeast Germany. *Ecology* 3:294–305. doi:10.1002/eco.108
- Nachabe, M.H. 2002. Analytical expressions for transient specific yield and shallow water table drainage. *Water Resour. Res.* 38(10):1193. doi:10.1029/2001WR001071
- Nagare, R., R. Schincariol, W. Quinton and M. Hayashi. 2011. Laboratory calibration of time domain reflectometry to determine moisture content in undisturbed peat samples. *Eur. J. Soil Sci.* 62:505–515. doi:10.1111/j.1365-2389.2011.01351.x
- Neff, E.L. 1977. How much rain does a rain gage gage? *J. Hydrol.* 35:213–220. doi:10.1016/0022-1694(77)90001-4
- Nungesser, M.K. 2003. Modelling microtopography in boreal peatlands: Hummocks and hollows. *Ecol. Modell.* 165:175–207. doi:10.1016/S0304-3800(03)00067-X
- Paavilainen, E., and J. Päivänen. 1995. Peatland forestry: Ecology and principles. *Ecol. Stud.* 111. Springer, Berlin. doi:10.1007/978-3-662-03125-4.
- Paquet, J., J. Caron, and O. Banton. 1993. In situ determination of the water desorption characteristics of peat substrates. *Can. J. Soil Sci.* 73:329–339. doi:10.4141/cjss93-035
- Pepin, S., A.P. Plamondon, and J. Stein. 1992. Peat water content measurement using time domain reflectometry. *Can. J. For. Res.* 22:534–540. doi:10.1139/x92-070
- Price, J.S. and S.M. Schlotzhauer. 1999. Importance of shrinkage and compression in determining water storage changes in peat: The case of a mined peatland. *Hydrol. Processes* 13:2591–2601. doi:10.1002/(SICI)1099-1085(199911)13:16<2591::AID-HYP933>3.0.CO;2-E
- Price, J.S., P.N. Whittington, D.E. Elrick, M. Strack, N. Brunet, and E. Faux. 2008. A method to determine unsaturated hydraulic conductivity in living and undecomposed moss. *Soil Sci. Soc. Am. J.* 72:487–491. doi:10.2136/sssaj2007.0111N
- Reynolds, W.D., D.E. Elrick, E.G. Youngs, and A. Amoozegar. 2002a. The soil solution phase: Field methods. In: J.H. Dane and G.C. Topp, editors, *Methods of soil analysis. Part 4. Physical methods.* SSSA Book Ser. 5. SSSA, Madison. p. 817–878. doi:10.2136/sssabookser5.4.c32
- Reynolds, W.D., D.E. Elrick, E.G. Youngs, H.W.G. Booltink, and J. Bouma. 2002b. The soil solution phase: Laboratory methods. In: J.H. Dane and G.C. Topp, editors, *Methods of soil analysis. Part 4. Physical methods.* SSSA Book Ser. 5. SSSA, Madison. p. 802–816. doi:10.2136/sssabookser5.4.c31
- Scharnagl, B., S. Iden, W. Durner, H. Vereecken, and M. Herbst. 2015. Inverse modelling of in situ soil water dynamics: Accounting for heteroscedastic, autocorrelated, and non-Gaussian distributed residuals. *Hydrol. Earth Syst. Sci. Discuss.* 12:2155–2199. doi:10.5194/hessd-12-2155-2015
- Scharnagl, B., J.A. Vrugt, H. Vereecken, and M. Herbst. 2011. Inverse modelling of in situ soil water dynamics: Investigating the effect of different prior distributions of the soil hydraulic parameters. *Hydrol. Earth Syst. Sci.* 15:3043–3059. doi:10.5194/hess-15-3043-2011
- Shibchurn, A., P.J. Van Geel, and P.L. Kennedy. 2005. Impact of density on the hydraulic properties of peat and the time domain reflectometry (TDR) moisture calibration curve. *Can. Geotech. J.* 42:279–286. doi:10.1139/t04-075
- Van der Ploeg, M., W. Appels, D. Cirkel, M. Oosterwoud, J.-P. Witte, and S. van der Zee. 2012. Microtopography as a driving mechanism for ecohydrological processes in shallow groundwater systems. *Vadose Zone J.* 11(3). doi:10.2136/vzj2011.0098
- van Genuchten, M.Th. 1980. A closed-form equation for predicting the hydraulic conductivity of unsaturated soils. *Soil Sci. Soc. Am. J.* 44:892–898. doi:10.2136/sssaj1980.03615995004400050002x
- von Post, L., and E. Granlund. 1926. *Södra Sveriges Torvtillgångar I* (Peat resources in southern Sweden I). Ser. C 335(19). Sveriges Geologiska Undersökning, Stockholm.
- Vrugt, J.A., and C.J.F. Ter Braak. 2011. DREAM_{SD}: An adaptive Markov chain Monte Carlo simulation algorithm to solve discrete, noncontinuous, and combinatorial posterior parameter estimation problems. *Hydrol. Earth Syst. Sci.* 15:3701–3713. doi:10.5194/hess-15-3701-2011
- Vrugt, J.A., C.J. Ter Braak, M.P. Clark, J.M. Hyman, and B.A. Robinson. 2008. Treatment of input uncertainty in hydrologic modeling: Doing hydrology backward with Markov chain Monte Carlo simulation. *Water Resour. Res.* 44. doi:10.1029/2007WR006720
- Vrugt, J.A., C.J.F. Ter Braak, C.G.H. Diks, B.A. Robinson, J.M. Hyman, and D. Higdon. 2009a. Accelerating Markov chain Monte Carlo simulation by differential evolution with self-adaptive randomized subspace sampling. *Int. J. Nonlinear Sci. Numer. Simul.* 10:273–290. doi:10.1515/IJNSNS.2009.10.3.273
- Vrugt, J.A., C.J.F. ter Braak, H.V. Gupta, and B.A. Robinson. 2009b. Equifinality of formal (DREAM) and informal (GLUE) Bayesian approaches in hydrologic modeling? *Stochastic Environ. Res. Risk Assess.* 23:1011–1026. doi:10.1007/s00477-008-0274-y
- Waddington, J.M., P.J. Morris, N. Kettridge, G. Granath, D.K. Thompson, and P.A. Moore. 2015. Hydrological feedbacks in northern peatlands. *Ecology* 8:113–127. doi:10.1002/eco.1493
- Wang, P., and S.P. Pozdniakov. 2014. A statistical approach to estimating evapotranspiration from diurnal groundwater level fluctuations. *Water Resour. Res.* 50:2276–2292. doi:10.1002/2013WR014251
- White, W.N. 1932. A method of estimating ground-water supplies based on discharge by plants and evaporation from soil: Results of investigations in Escalante Valley, Utah. USGS Water Supply Pap. 659-A. US Gov. Print. Office, Washington, DC.
- Wollschläger, U., T. Pfaff, and K. Roth. 2009. Field-scale apparent hydraulic parameterisation obtained from TDR time series and inverse modelling. *Hydrol. Earth Syst. Sci.* 13:1953–1966. doi:10.5194/hess-13-1953-2009